ELSEVIER

Polymer 40 (1999) 5751–5759

polymer

Morphology of poly(chloro-*p*-xylylene) CVD thin films

Jay J. Senkevich*, Seshu B. Desu

Virginia Technic Institute, Department of Materials Science and Engineering, 213 Holden Hall, Blacksburg, VA 24061-0237, USA

Received 22 September 1997; received in revised form 1 November 1998; accepted 3 November 1998

Abstract

Poly(chloro-*p*-xylylene) thin films are shown to have a changing morphology as a function of deposition temperature from spectroscopic ellipsometry and X-ray diffraction measurements. At lower deposition temperatures, the as-deposited polymer exhibited negative birefringence attributed to the presence of amorphous conformationally disordered polymer chains. As the deposition temperature was increased the polymer chains became more conformationally ordered resulting in an increase in the thin film's birefringence. At higher deposition temperatures, above the polymer's T_g evidence of crystallinity was apparent from X-ray diffraction results. The increase in the thin film's birefringence may be attributed to the thermodynamic driving force for crystallization causing the plane of the phenyl group to orient more perpendicular to the plane of the substrate, evidently the more stable conformation for poly(chloro-*p*-xylylene). After an inert post-deposition anneal at 210°C for 2 h, the thin films deposited at lower temperatures showed evidence of higher crystal quality than the above T_g deposited films because of a smaller *d*-spacing. A decrease in the full width half max of the X-ray diffraction peak was attributed to a large increase in the crystallite size, larger for the films deposited at higher temperatures as a result of a greater degree of crystallinity present in those films as-deposited. Further, comparisons are made between the as-deposited and post-deposition annealed samples in terms of stress, crystalline disorder and crystallite size. In addition, from differential scanning calorimetry measurements, the glass transition temperature of poly (chloro-*p*-xylylene) was 35°C–36°C and 44°C at heating rates of 0.2°C/min and 5°C/min.

Keywords: Morphology; CVD; Poly(chloro-*p*-xylylene)

1. Introduction

Much attention was focused on the applications of the parylene polymers (Fig. 1) because of their high solvent resistance, low dielectric constant, good barrier properties, biocompatibility, and their ability to be deposited by chemical vapor deposition (CVD) [1–6]. Poly(chloro-*p*-xylylene) (PPXC), in particular, has a high resistance to permeability of common gases such as H_2O, N_2, and O_2 and also exhibits a high elastic modulus [7]. With its exceptional properties, PPXC was utilized as an ultrapure highly conformal CVD thin film or coating for many and varied applications. However, fundamental studies of the parylenes have been limited. A basic understanding is needed to correlate the structure–property relations in order to fully exploit the properties of the PPXC and the parylene polymer family. This is especially true for the fluorinated parylenes which are the prime candidate materials for interlayer dielectrics to reduce RC-delay, power consumption, and cross-talk in ULSI devices [2,3].

A long-standing controversy exists in relation to the glass transition temperatures of the parylene polymers [8–11]. As a result of the presence of the flexible aliphatic carbon–carbon single bonds in all the parylene polymers, their T_g's are near room temperature. The possible difference for PPXC's T_g of 80°C versus one of $\backsim$ 40°C is significant because many applications generate heat internally, such as ULSI devices, and ambient conditions may reach such temperatures. Above its T_g, a polymer's permeability, mechanical, electrical, thermal, and optical response may change significantly affecting its properties and, for example, device reliability and performance. Previous reports for the T_g of the PPXC homopolymer were 50°C, 70°C, and 80°C, [8–10]. The study here attempts to elucidate this controversy over PPXC's T_g by using differential scanning calorimetry (DSC), and substantiate further with X-ray diffraction (XRD). Further, the finding of T_g for PPXC is used to make conclusions about structural aspects of PPXC's crystalline phase as-deposited as a function of deposition temperature and then after a post-deposition anneal. XRD may indicate the degree of stress, crystal disorder, and crystallite size for the thin films in terms of the full width half max (FWHM), *d*-spacings, and peak height of the diffraction planes.

Spectroscopic ellipsometry is used here as a complemen-

* Corresponding author. Fax: 001 540 231 8919.
E-mail address: jsenkevi@ vt.edu (J.J. Senkevich)

0032-3861/99/$ - see front matter
PII: S0032-3861(98)00793-9

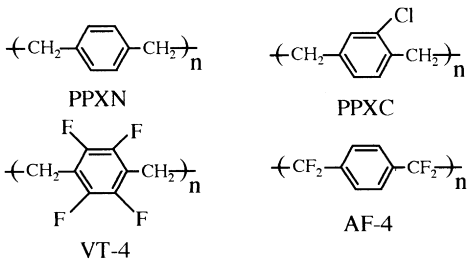

Fig. 1. Some representative parylene polymers.

tary method with XRD to understand the overall conformational ''orderness'' of the thin films. Spectroscopic ellipsometry which measures the optical birefringence of the polymer thin films is not selective to either the amorphous or crystalline phases, but instead is sensitive to relative position of the benzene ring as a part of PPXC's repeat unit. Finally, a simple explanation is given as to why CVD polymers exhibit a decrease in deposition rate as the deposition temperature is increased.

2. Experimental

Fig. 2 shows a schematic of the custom-built CVD reactor with separate sublimation, pyrolysis, and near-room temperature deposition chambers [8]. DPXC was sublimed at 119°C to achieve a deposition rate of 3.7 to 22.5 nm/min, depending on the deposition temperature and to a lesser extent on the surface conditions of the substrate. The pyrolysis chamber itself was heated to 600°C, converting the dimer into the monomer diradical reactive intermediate as shown in Fig. 3. Water circulated through copper tubing surrounding the deposition chamber to achieve deposition temperatures of −3°C to 90°C measured in situ with a thermocouple. The pressure of all the depositions was 0.105–0.120 Torr and lasted between 15 and 60 min, depending on the thickness of the film desired. The substrates used for depositing the PPXC films were (111) silicon for optical and XRD characterization and NaCl polycrystalline sintered substrates to make free-stranding films for T_g determination.

The glass transition temperatures of the PPXC homopolymer were obtained by using a Perkin-Elmer DSC-7 differential scanning calorimeter. The PPXC thin films were grown on polycrystalline sintered NaCl substrates, which were subsequently dissolved in H_2O until the films floated. The resulting films were then placed onto an aluminum foil and heated upto 130°C for at least 2 h, to evaporate any residual water. DSC samples were then made with the free standing films. The DSC samples were heated to 115°C for 30 min before cooling to room temperature to evaporate any residual H_2O. The samples were then heated at 10°C/min to find the general region of the T_g. After finding the general region of the T_g, the samples were either heated at 0.2°C/min or 5°C/min two times in order to ensure reproducibility and to make sure that no residual H_2O existed. X-ray diffraction data was obtained using a Scintag XDS-2000 (Sunnyvale, California) X-ray diffractometer with Cu Kα radiation of 1.5418 Å. Scans were made from 10 to 26° 2θ for the PPXC thin films.

The thickness and optical characterization was carried out by using a variable angle spectroscopic ellipsometer (VASE) from the J.A. Woollam Company, Lincoln, Nebraska. The wavelength of light used was 400–1000 nm and three angles from the normal to the sample were used: 70°, 75° and 80°. The parameters obtained from VASE are delta and psi, the trigonometric parameters which characterize the ellipsoid produced after linearly polarized light is ellipsometrically polarized after thin film interaction. An anisotropic Cauchy model was fitted to delta and psi generating thickness and dispersion curves for the out-of-plane and in-plane indices of refraction for each PPXC thin film. The thickness of the PPXC polymer thin films used for optical characterization varied from 82 to 568 nm.

3. Deposition rate versus deposition temperature

There exists a competition in the ultimate deposition rate of the parylenes between adsorption of the reactive intermediate and the polymerization rate of the polymer. The

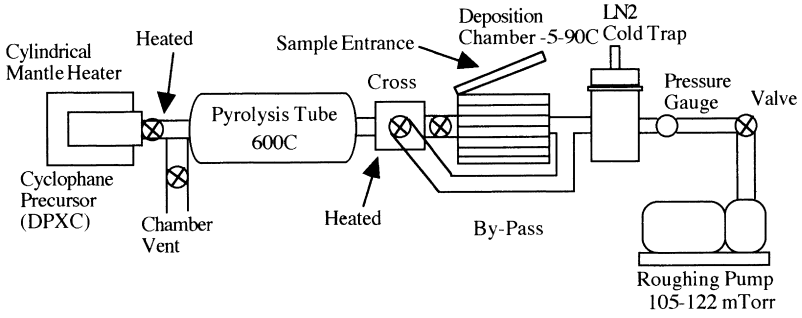

Fig. 2. Custom built chemical vapor deposition reactor.

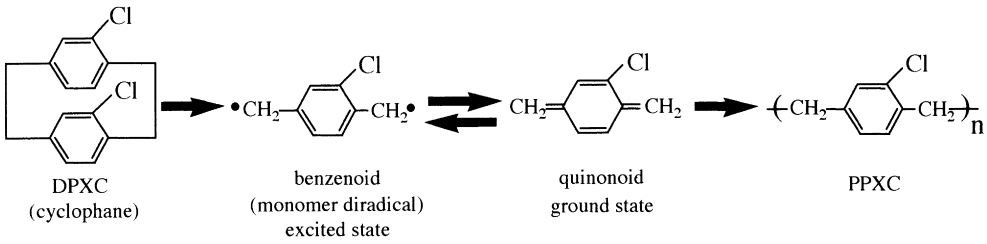

Fig. 3. Gorham process used to synthesize PPXC from the dimer precursor.

reaction sequence is shown as:

$$\text{Dimer/precursor} \rightarrow \cdot M\cdot,$$

$$\cdot M\cdot \xrightarrow{k_A} (\cdot M\cdot)_A,$$

$$2(\cdot M\cdot)_A \xrightarrow{k_p} \cdot M\text{–}M\cdot,$$

where the dimer is the cyclophane precursor used in this study, but other precursors may also be used, $\cdot M\cdot$ is the monomer diradical reactive intermediate, the subscript A denotes the adsorbed species, k_A is the rate constant for $\cdot M\cdot$ to be physisorbed onto the substrate, and k_p is the rate constant for polymerization. This constant can be broken down into the rate constants for initiation and propagation (no termination occurs for CVD polymers), but for simplicity only the rate of polymerization will be considered. The rate determining step in the earlier sequence of reactions, albeit physisorption of the monomer diradical or the polymerization of the intermediate, is determined in large part by the temperature of deposition if the concentration of the intermediate and the pressure of the system is kept constant.

The two processes have a markedly different temperature dependence, namely for polymerization an activation energy E_A exists such that the Arrhenius equation can be used.

$$\text{Rate of polymerization} = A\exp(-E_A/RT), \quad (1)$$

where A is the pre-exponential factor which is related to the collision density and steric effects of the reacting monomeric species. The collision density is intimately related to the rate of adsorption and is the number of monomeric collision per unit volume per unit time. Further, the two reacting molecules need to be in the requisite positions or geometries for a successful reaction to take place and hence the steric factor. For the typical chemical reaction, albeit exothermic or endothermic, its rate increases with an increase in the temperature of the system. The activation energy is normally considered an energy barrier and has to be positive to be physically meaningful.

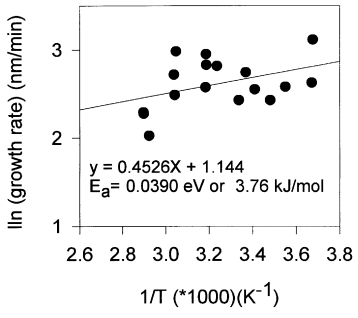

Fig. 4. Arrhenius plot for the deposition of PPXC at a sublimation temperature of 119°C.

Adsorption processes can be shown to be Arrhenius-like, but with an entirely different physical interpretation [12–13].

$$\text{Rate of absorption} = k_{desorb} P\, b_0 \exp(Q/RT) \quad (2)$$

where k_{desorb} is the rate constant for desorption, $k_{desorb} \backsim 0$ for chemisorption and k_{desorb} is significant for physisorption. P is the pressure of the system, b_0 is a function of the molecular weight of the gas, the temperature of the substrate, and other less significant factors for the treatment here, and finally Q is the energy of absorption.

At higher substrate temperatures (>0°C), the rate of absorption is rate limiting and hence there is a decrease in deposition rate with an increase in deposition temperature. At very low deposition temperatures, e.g. LN_2 temperatures, the absorption rate is significantly greater than the polymerization rate thus resulting in a different temperature dependence and film morphology [14]. Fig. 4 shows an Arrhenius-like plot for the growth rate versus deposition temperature. The scatter in the data is primarily due to the use of a ''hot-walled'' CVD reactor and the surface conditions of the substrate. Quotations are used with hot-walled CVD reactor, as this term is normally reserved with metallorganic-CVD reactors which are heated to relatively high temperatures >500°C (unlike the present case) and where deposition occurs on the substrate and the walls of the reactor concurrently. Of course, MOCVD of ceramics and CVD of polymers occur by entirely different deposition mechanisms which will not be discussed any further. The polymerization in Fig. 4 is mass-transport controlled. This implies that significant polymer is deposited at the top of the deposition chamber reducing the mass flux to the surface of the substrate where absorption and subsequent polymerization occurs. At lower deposition temperatures, more polymer is deposited at the top of the hot-walled CVD reactor leaving

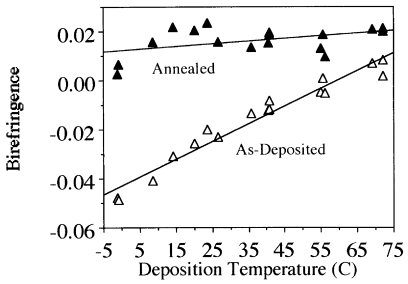

Fig. 5. Optical birefringence of PPXC thin films as-deposited and after a 210°C anneal for 2 h.

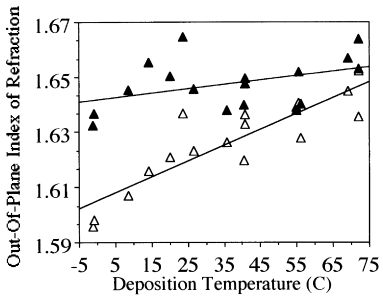

Fig. 7. Out-of-plane index of refraction of PPXC thin films as-deposited and after a 210°C anneal for hours.

less polymer, which is able to be polymerized, at the substrate surface.

However, a positive slope is apparent throughout Fig. 4 which implies adsorption is the dominant process. For PPXC, 90°C is normally considered the threshold temperature, above which little or no polymerization can occur because of the lack of monomer/substrate interaction, i.e. no absorption takes place. At higher temperatures, the slope of the line (converted to an energy of absorption) was 25.6 ± 8.7 kJ/mol on a per mole basis or 0.275 ± 0.090 eV on a per molecule basis. Physisorption processes are considered to dominate in the general region 8–38 kJ/mol. Larger absorption energies equal or greater than ∽ 84 kJ/mol are reserved for chemisorption processes [12]. The monomer diradical (benzenoid) parylene intermediate which exhibits an energy of absorption near the upper range of physisorption is understandable as free-radical containing atoms or molecules are highly reactive, interacting strongly with most of their nearest neighbor species. A previous report of the absorption (wrongly claimed as a negative activation energy) was 26.0 kJ/mol, which is similar to the value reported here [31]. As there is a relatively large error in the absorption energy reported here, it may be little more than coincidence that the two values are so similar.

4. Birefringence as related to morphology

Fig. 5 shows the birefringence of PPXC as a function of deposition temperature and after a 210°C post-deposition anneal for 2 h. The birefringence is defined as:

$$\Delta = n_{\text{out-of-plane}} - n_{\text{in-plane}}, \tag{3}$$

where $n_{\text{out-of-plane}}$ is the out-of-plane index of refraction (perpendicular to the plane of the substrate, Fig. 6) and $n_{\text{in-plane}}$ is the in-plane index of refraction (defined by the plane of the substrate, Fig. 7). In order to interpret the birefringence results, the anisotropic molecular polarizability of the PPXC repeat unit should be characterized as it is the fundamental unit of the macromolecule and hence defines the optical anisotropy of the thin film. Benzene, similar to the PPXC repeat unit, has a rather large anisotropic molecular polarizability of $\Delta\alpha = 5.62$ Å^3. The polarizability of the benzene ring is greatest in the plane of the ring 12.27 Å^3 as opposed to the polarizability perpendicular to the plane of the ring 6.65 Å^3 [15,16]. With the addition of chlorine to benzene, the mean molecular polarizability increases from 10.4 to 12.5 Å^3 as chlorine is more highly polarizable compared to hydrogen. The addition of chlorine increases both the out-of-plane (7.58 Å^3 versus 6.65 Å^3) and the in-plane molecular polarizabilities compared to benzene. However, the plane of the chlorobenzene ring no longer possesses three-fold symmetry like benzene, therefore, it has different *x*-axis and *y*-axis in-plane polarizabilities, both of which are large compared to benzene (15.93 Å^3 versus 12.27 Å^3 along the axis containing the chlorine atom and 13.24 Å^3 versus 12.27 Å^3 versus the non-chlorine containing axis). Thus, chlorobenzene has two anisotropic molecular polarizabilities 8.35 Å^3 with respect to the in-plane axis containing the chlorine atom and 5.66 Å with respect to the in-plane axis without the chlorine atom which is nearly the same as that of benzene 5.62 Å^3 [17].

Chlorobenzene is then like benzene, except that it is more polarizable and has a large anisotropic molecular polarizability allowing PPXC's repeat unit to be more birefringent with respect to the same orientation of its hydrocarbon cousin, PPXN's repeat unit. Relating the earlier discussion to the birefringence results, when the plane of the phenyl group is tilted perpendicular to the substrate the out-of-plane index of refraction is large (positive birefringence) because of the high in-plane polarizability of the phenyl group. Likewise, if the plane of the phenyl group is parallel with the plane of the substrate, then the in-plane index of refraction

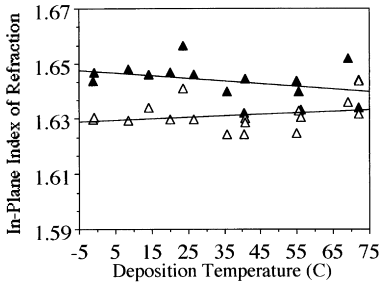

Fig. 6. In-plane index of refraction of PPXC thin films as-deposited and after a 210°C anneal for hours.

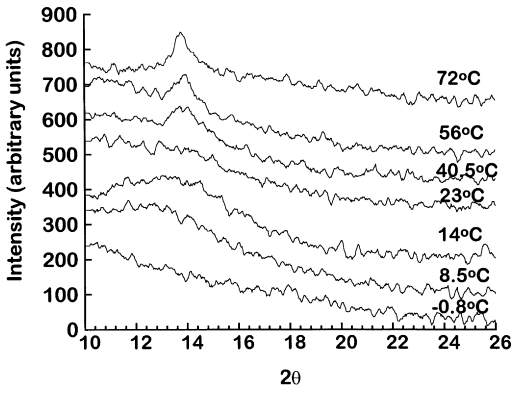

Fig. 8. XRD spectra for PPXC in the as-deposited condition. The peak represents the (020) plane of the monoclinic unit cell.

would be high (negative birefringence). As PPXC crystallizes, its phenyl group is slightly tilted perpendicular to the substrate in a chain-folded morphology unlike PPXN whose phenyl group lies preferentially parallel to the plane of the substrate [18].

Fig. 5 shows a linear increase in the birefringence of PPXC with increasing deposition temperature. At low deposition temperatures, the plane of the phenyl group is more parallel to the plane of the substrate (the chain is conformationally disordered) and the polymer is amorphous according to XRD (Fig. 8) [19]. However, increasing the deposition temperature lead to an increase in the thin film's birefringence probably because of more energy available for crystallization. This results in a more ordered polymeric chain, yet no crystalline unit cell can be defined until the polymer is deposited above its T_g. This hypothesis is confirmed by the decrease in the FWHM values for the PPXC films deposited from 40.5°C to 72°C where a crystalline unit cell can be defined. Such a decrease is directly related to the presence of larger crystallites indicative of a greater degree of crystallization (Table 1). PPXC thin films deposited at 25°C and 80°C and annealed at 200°C for 30 min resulted in percent crystallinities of 51% and 73%. Evidently, the deposition temperature has a large impact on PPXC's morphology as-deposited and also after post-deposition anneals.

At a deposition temperature of 40.5°C, a crystalline phase is evident for PPXC according to XRD (Fig. 8). PPXC's glass transition temperature likely exists between 23°C and 40.5°C as crystallization is not possible below the T_g at low precursor sublimation rates. This is only true when polymerization and then subsequent crystallization takes place, which occurs at higher deposition temperatures, where physisorption is the rate limiting step for the deposition rate [14]. After a 210°C post-deposition anneal for 2 h, the PPXC thin films had nearly the same positive birefringence, however, a slight slope is evident. This slight slope may be caused by a difference in the degree of crystallization as, like the as-deposited films, the post-deposition annealed films show a decrease in their FWHM with increasing deposition temperature (Table 1).

5. X-ray diffraction as related to morphology

Table 1 shows the results for XRD data, including the FWHM and *d*-spacings, both as-deposited and after a 210°C post-deposition anneal. The FWHM is a function of the stress state of the film, degree of disorder in the crystallographically defined unit cell (paracrystallinity), and the crystallite size. While the change in *d*-spacings are primarily because of paracrystallinity and to a lesser extent because of the stress state of the film. For films thicker than ~ 100 nm, the crystallite size is reflective of the diameter of the polymer spherulite, a complex three-dimensional structure composed not simply of crystalline polymer, but also of amorphous polymer with a chain-folded morphology. For films thinner than ~ 100 nm, the crystallite size is reflective of the diameter of a two-dimensional structure, probably to a degree composed of chain-folded morphology. However, as the film becomes thinner a chain-extended morphology develops resulting in a reduced degree of crystallization [20–22].

Previous work has shown that the magnitude of the stress for PPXC increases after thermal anneal as measured by the change in the radius of curvature of the PPXC films deposited on silicon. The stress was initially compressive (−8 MPa) and then became nearly a constant and tensile after heating the thin film polymer above 200°C, then cooling it back to ambient conditions (35 MPa) [23]. The nearly

Table 1
X-ray diffraction data

Deposition temperature	Film thickness	As-deposited			Annealed at 210°C			ΔFWHM
		d-spacing	°2θ	FWHM (°2θ)	*d*-spacing	°2θ	FWHM (°2θ)	
−0.8°C	462	–	–	–	6.199	14.28	0.73	–
8.5°C	441	–	–	–	6.199	14.28	0.67	–
14°C	375	–	–	–	6.219	14.23	0.65	–
23°C	239	–	–	–	6.219	14.23	0.66	–
40.5°C	467	6.38	13.9	1.1	6.239	14.18	0.62	−0.5
56°C	504	6.37	13.9	1.0	6.259	14.14	0.59	−0.4
72°C	383	6.41	13.8	0.7	6.300	14.05	0.54	−0.2

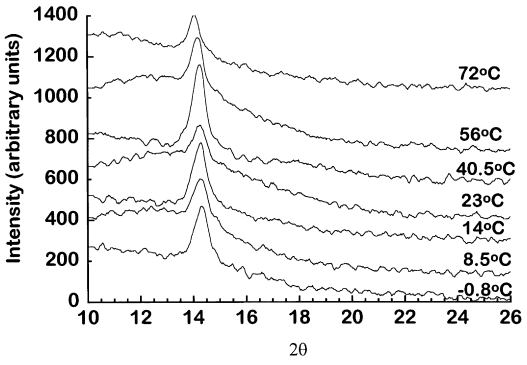

Fig. 9. XRD spectra for PPXC after a 210°C 2 h anneal.

constant stress is caused by heating the polymer significantly above its T_g where stress relaxation could occur (within the amorphous phase), then a subsequent tensile stress developed owing to the difference in coefficient of thermal expansion (CTE) between the silicon substrate ($2.6 \times 10^{-6}\,K^{-1}$) and the PPXC thin films ($35 \times 10^{-6}\,K^{-1}$) [24,25]. By differentiating Bragg's law and assuming the material to be isotropic, one can obtain [26]:

$$b = -2(\sigma/E)\tan\theta, \tag{4}$$

where b is the additional line broadening caused by non-uniform strain, in the present case because of the CTE mismatch between the silicon substrate and PPXC thin film. σ is the measured stress of the film (by independent experiments), θ is the center of the diffraction peak in degrees and E is the modulus of elasticity. Using $\theta = 7°$ {the (020) diffraction peak from the monoclinic unit cell of PPXC}, $E = 3.2$ GPa [24] and $\sigma = 0.035$ GPa for PPXC, one obtains an increased line broadening of $b = 0.308°2\theta$, which is significant.

The effect of stress on the change in d-spacings for polymers is much less significant. The stress for any material through some simple derivations is given by:

$$\sigma = K_1(\Delta 2\theta), \tag{5}$$

where σ is the stress of the material, which can be uniform or non-uniform, $\Delta 2\theta$ is the change in the peak position and K_1 is the stress constant given by:

$$K_1 = E\cot\theta/2(1+\nu)\sin^2\Psi, \tag{6}$$

where E is Young's modulus, ν is the Poisson's ratio, and Ψ is the angle between the two plane-measurements and is normally given by 45°. Using the previous values for the FWHM treatment and $\nu = 0.33$ for a typical semicrystalline polymer, a value of 19.6 GPa was obtained for K_1. With a stress of 0.035 GPa, a change in the diffraction peak position is $0.0018°2\theta$ which is too small to be detected. The shift in the 2θ values (Table 1) is then owing to paracrystallinity within the PPXC unit cell which is not unexpected as the repeat unit of PPXC is asymmetrical and its unit cell is monoclinic, possessing a low degree of symmetry. The degree to which the paracrystallinity affects the FWHM values will not be determined here, however, an increase in the ''orderness'' of the crystal phase should: decrease the FWHM and the d-spacings for each X-ray diffraction plane [27].

An increase in crystallite size is the primary reason for the reduction in FWHM values after the post-deposition anneal, considering the earlier discussion and the large increase for each thin film X-ray diffraction plane peak (Fig. 8 compared to Fig. 9). Above 40°C, crystallization is evident in the as-deposited films and the peak corresponds to the (020) diffraction plane of the monoclinic unit cell with cell dimensions $a = 5.96$ Å; $b = 12.8$ Å, 12.7 Å, 12.8 Å; $c = 6.66$ Å; $\beta = 135.2°$, where $d = b/2$($d = d$-spacing, $b = b$-axis of the monoclinic unit cell) for the deposition temperatures of 40.5°C, 56°C, and 72°C respectively. These values correspond well with what Murthy and Kim [28] and Isota et al. [29] found for PPXC, namely $b = 12.8$ Å. After a post-deposition anneal, the films deposited at 40.5°C and above show a reduction in the d-spacing and hence a reduction in the b-axis of the monoclinic unit cell lending to a more stable crystalline phase. The FWHM is large in the as-deposited films grown above 40.5°C owing to the presence of small crystallites and a high degree of crystalline disorder present within the PPXC thin films. Increasing the deposition temperature above 40.5°C leads to smaller FWHM values because of more thermal energy available for crystallization resulting in larger more ordered polymer crystallites.

Some trends are apparent from Table 1. The PPXC thin films deposited at 40.5°C, 56°C, and 72°C experience nearly the same shift in their diffraction peak 0.14, 0.11, and 0.11 Å respectively. This may be expected as the same degree of thermal energy is available for further crystallization. These same as-deposited films exhibited a decrease in their FWHM as the deposition temperature was increased because of an increase in the degree of crystallization. The subsequent decrease in the FWHM values after the films were annealed was less for the films deposited at higher initial temperatures because of the high initial degree of crystallinity existing in these films. Of more interest is the trend of an increase in the d-spacings after the 210°C post-deposition anneal for the thin films deposited at higher temperature from −0.8°C to 72°C. As the deposition temperature is lowered and the films are subsequently annealed, the d-spacings are smaller and thus a more ordered monoclinic unit cell is formed. Further, as a result of their larger FWHM values, the films deposited at lower temperatures which were then subsequently annealed contain smaller crystallites than those films deposited at higher deposition temperatures. This, of course, assumes that all the films possess nearly the same stress state within their crystalline phase, which is probable. The stress state within the polymer's amorphous phase may not be the same and should be highly dependent on the polymer crystallite's morphology and the thickness of the film.

After annealing, the birefringence exhibits a slight

Table 2
Glass transition temperature of PPXC

T_g (°C)	ΔC_p (J/°Cmol)	Rate	Method	Study
35–36	0.87	0.2°C/min	DSC	This Study
44	0.43	5°C/min	DSC	This Study
50	0.20	10°C/min	DSC	Alpaugh/Morrow [9]
70	–	?	?	Gilch/Wheelwright [10]
80	–	10% strain/min	Secant modulus	Gorham [8]

slope as a function of the deposition temperature, most likely because of the difference in the film's degree of crystallization. The relatively large change in the low temperature deposited thin film's birefringence after post-deposition anneal is reflective of the PPXC polymeric chain becoming conformationally ordered and a large increase in the film degree of crystallization. This increase in the polymer chain orderness is directly related to the increase in the degree of crystallization. An obvious concern exists in relation to Table 1, namely after a post-deposition anneal at 210°C for 2 h, the PPXC thin films deposited at −0.8°C–72°C do not show the same *d*-spacings. As earlier mentioned, the change in *d*-spacings for the PPXC polymer thin film represents the degree of paracrystallinity of the monoclinic unit cell. The consequence of a larger *d*-spacings for a polymer crystallite as compared to the one with a smaller *d*-spacing is a less stable polymer crystallite manifested as the polymer crystallite exhibiting a lower melt transition. In the case of PPXC, at its melt transition, film disruption occurs because of the chlorine containing benzene ring rotating which affects its nearest neighbor's lattice position and hence the disruption of the polymer crystallite. Therefore, this hypothesis can be easily tested with X-ray diffraction or optical methods as the polymer film at its melt transition will become amorphous and isotropic.

However, why should such structural differences exist for PPXC as a function of deposition temperature? The answer maybe the glass transition temperature which, according to the XRD data, is between 23°C and 40.5°C. Chemical vapor polymerization (CVP) above the polymer's solid state T_g can easily result in polymer crystallization. As the deposition temperature is increased a greater degree of crystallization should take place. Despite the conventional wisdom of solid state thermodynamic transitions regarding the glass transition; namely, no crystallization should be able to take place below the polymer's T_g. This may not be necessarily the same with regard to the processes which underlie CVP, in which concurrent polymerization and crystallization may take place. At low deposition rates, not enough localized heating exists to result in any substantial crystallization and hence all that can be expected is the formation of crystal nuclei. The crystal nuclei do not have a well defined crystal structure like when they transform to a small polymer crystallite exhibiting a chain-folded morphology with a defined crystalline unit cell.

After a small polymer crystallite is formed, it becomes much like a template for further polymer crystallization. The higher energy crystallization process is for a disordered crystallite to go through chain reorganization to form a more perfect crystal. More likely, amorphous polymer chains will crystallize outward from the initial disordered crystallite resulting in an apparent increase in average crystal quality. Therefore, when annealed these films go through a nucleation and growth process to form more perfect (lower *d*-spacing) crystals but their crystallites are smaller owing to less time available for growth as compared to the films deposited at higher temperatures.

6. Glass transition temperature

Accurate determination of the glass transition for the parylene polymers and more specifically poly (chlore-*p*-xylylene) is important because they have the T_g's near-room temperature [7]. What is more, PPXC's T_g is near the same temperature at which it is often deposited, which may effect its as-deposited morphology and its subsequent morphology after post-deposition anneal, as discussed earlier. The morphology in turn affects the physical properties of the polymer thin film such as its elastic modulus, electrical properties such as its dielectric loss, and optical properties such as its optical anisotropy.

A reliable measurement of T_g necessitates elimination of any residual solvent as typically far less than a mole percent of solvent can significantly lower the T_g [30]. However, PPXC is very impervious to moisture and therefore the lowering of its T_g owing to solvent uptake is less of a concern. To ensure that no solvent existed in the free-standing PPXC films, they were heated to 130°C for 2 h, then to 115°C for 30 min within the DSC.

Under most circumstances, the cooling rate from the melt must be large to ensure that the polymer is amorphous. However, in the case of PPXC heating above the melting point at 293–294°C ($T_{deposition}$ = 14°C, as measured in this study) resulted in an amorphous material with a largely different morphology compared to a typical glassy polymer regardless of the cooling rate (<1°C/min). This phenomena was also found in a previous study and by Scarrow and Gunn [19]. What is more, semicrystalline polymers exhibit an increase in their T_g, a larger T_g range and a decrease in ΔC_p making T_g determination more difficult as less

amorphous material exists to contribute to the T_g. Typically, with the use of DSC to determine the T_g, a minimum sample weight of $\sim$ 10 mg should be used if the polymer is amorphous and more if it is semicrystalline. In the study here, typical sample weights were $\sim$ 3 mg, which translates to a $\sim$ 3 μm film with a substrate surface area of 10 cm^2 and a density of 1 g/cm^3 for the polymer film, which is no longer a thin film but a coating. Less sample mass would render the DSC instrument less sensitive to the T_g. To remedy this concern, the PPXC free-standing films were heated to above their melt transition rendering them amorphous. Then, the DSC scans were run at lower rates to allow the transition to be resolved.

Table 2 compares the T_g values as measured by the inflection point, the change in the heat capacity ΔC_p, and the scan rate. The only previous determination of PPXC's T_g which utilized DSC and was well characterized was carried out by Alpaugh and Morrow [9]. Gorham first characterized PPXC's T_g by the use of the secant modulus method. However, this method suffers from poor sensitivity to the T_g and therefore a higher T_g would be expected. The results found here correspond well to Alpaugh and Morrow's study, in that a lower scan rate when heating the polymer sample should reduce the T_g and increase ΔC_p. Without a distribution of relaxation times for the polymer, the T_g should be a rate independent second-order thermodynamic transition. However, with a distribution of relaxation times for the amorphous phase of the polymer, the scan rate affects the T_g, range of T_g, and ΔC_p. Higher scan rates allow less time for relaxation to occur and thus a higher T_g, a broader T_g, and a lower ΔC_p should be evident.

7. Conclusions

PPXC exhibited a complex morphology as a function of deposition temperature, which subsequently influenced the morphology of the annealed film. Most important, optical birefringence was sensitive to the degree of crystallization which existed within the polymer thin films. Whereas, X-ray diffraction could draw conclusions about the morphology of the crystal phase of the polymer thin films. The birefringence results showed a negative birefringence for the polymer thin films deposited at low temperature, linearly increasingly until the thin film became positively birefringent at higher deposition temperatures ($>$60°C). The increase in the optical birefringence was because of an increase in the electronic polarization perpendicular to the substrate. This resulted from the change in the relative orientation of the phenyl group caused by a higher degree of polymer chain conformational order reflective by an increase in the degree of crystallization.

Analyzing the change in the FWHM and *d*-spacing values for the XRD diffraction plane peak, conclusions could be drawn in terms of the morphology of the PPXC thin films. Most significant, larger polymer crystallites of a lower degree of crystalline order existed within the polymer thin films deposited at higher temperatures both as-deposited and after a post-deposition anneal. Thus, after post-deposition anneal the PPXC thin films do not possess the same morphology, which may affect the resulting properties of the thin films. Care should then be taken to control the thermal history of the polymer thin films which affects their degree of crystallization, crystallite size, paracrystallinity, film stability and possibly their stress state. These structure/property relations are not easy to develop but this investigation should give some initial findings and basic data relevant to understanding polymer thin films.

Finally, the glass transition temperature for PPXC was 35–36°C at a scan rate of 0.2°C for the as-deposited polymer deposited at −0.8°C to 72°C. The T_g increased to 44°C at a scan rate of 5°C/min and the ΔC_p dropped from 0.87 to 0.43 J/°C mol. This findings corresponded well with the previous study by Alpaugh and Morrow.

References

[1] Pyle J. Machiene Design 1993:77–79.
[2] Dabral S, Zhang X, Wu XM, Yang G-R, You L, Lang CI, Hwang K, Cuan G, Chiang C, Bakhr H, Olson R, Moore JA, Lu T-M, Mcdonald JF. J Vac Sci Technol B 1993;11(5):1825–1832.
[3] Wary J, Olson RA, Beach WF. DUMIC Conference, 1996:207–213.
[4] Murarka SP. Solid State Technol 1996:83–90.
[5] Tanioka A, Fukushima N, Hasegawa K, Miyasaka K, Takahashi NJ. Appl Polym Sci 1994;54:219–229.
[6] Yamagishi FG. Thin Solid Films 1991;202:39–50.
[7] Greiner A. Polym Mater Encylopedia. In: Salamone JC, editor. Boca Raton: CRC Press, 1996:7171–7180.
[8] Gorham WF. J Polym Sci A-1 1966;4:3027–3039.
[9] Alpaugh WA, Morrow DR. Thermochim Acta 1974;9:171–204.
[10] Gilch HG, Wheelwright WL. J Polym Sci A-1 1966;4:1337–1349.
[11] Kirkpatrick DE, Wunderlich B. Makomol Chem 1985;186:2592–2607.
[12] Adamson AW. Physical chemistry of surfaces. New York: John Wiley and Sons, 1990:591–681.
[13] Langmuir I. J Phys Chem Soc 1911;40:1361.
[14] Gaynor JF. Electrochem Soc Proc 1997;97-98:176–185.
[15] Dewar MJS, Stewart JJP. Chem Phys Let 1984;111:416–420.
[16] Rudd JF, Gurnee EF. J Polym Sci A 1963;1:2857–2867.
[17] Denbigh KG. Trans Faraday Society 1940;36:936–948.
[18] Senkevich JJ, Desu SB. Semicondutor Int 1998;21:151–156.
[19] Scarrow RK, Gunn EE. Proc JOWOG-28-A: Organic coatings, 1987:61.
[20] Frank CW, Rao V, Despotopoulou MM, Pease RFW, Hinsberg WD, Miller RD, Rabolt JF. Science 1996;273:912–915.
[21] Despotopoulou MM, Frank CW, Miller RD, Rabolt JF. Macromolecules 1996;29:5797–5804.
[22] Escleine JM, Monasse B, Wey E, Haudin JM. Coll and Polym Sci 1984;262:366–373.
[23] Dabral S, Van Etten J, Apblett C, Yang GR, Ficalora P, McDonald JF. Mat Res Soc Symp Proc 1992;239:113–117.
[24] Beach WF, Lee C, Bassett DR, Austin TR, Olson RA. Encycl Polym Sci Technol New York: Wiley, 1989, vol. 17, pp. 990–1025.
[25] Sze SM. Physics of semiconductor devices. New York: John Wiley and Sons, 1981.
[26] Cullity BD. Elements of X-ray diffraction. Reading MA: Addison-Wesley, 1978.

[27] Kakudo M, Kasai N. X-ray diffraction by polymers. Amsterdam: Elsevier, 1972:111–133.
[28] Isoda S, Ichida T, Kawaguchi A, Katayama K-I. Bull Inst Chem Res Kyoto Univ 1984;61(3):222–228.
[29] Murthy NS, Kim H. Polymer 1984;25:1093–1096.
[30] Jenckel E, Heusch R. Kolloid Z 1953;130:19.
[31] Alexandrova L, Vera-Graziano R. Polym Mater Encylopedia. In: Salamone JC, editor. Boca Raton: CRC Press, 1996:7180–7189.